

## Carboberyllation: addition of organoberyllium species to alkenes and alkynes. A comparison with carboboration.

Terri E. Field-Theodore,<sup>a</sup> Shannon A. Couchman,<sup>a</sup> David J. D. Wilson<sup>a\*</sup> and Jason L. Dutton<sup>a\*</sup>

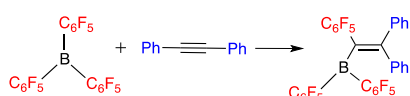
been investigated The potential for carbometallation reactions between organoberyllium and model alkenes and alkynes has in a computational study. Results indicate that barriers for carbometallation reactions between  $\text{BeR}_2$  and alkynes are as low as 100 kJ/mol, and much lower than corresponding reactions with  $\text{MgR}_2$ . In contrast to carboboration reactions with  $\text{BR}_3$ , with organoberyllium 1,2-addition is favoured over 1,1-addition. It is concluded that carbometallation reactions with beryllium are likely feasible, and that the reaction between  $\text{BePh}_2$  and alkynes provides the best opportunity for the first experimental observation of carboberyllation.

### Introduction

Addition to unsaturated C-C bonds is one of the fundamental reactions of organic chemistry, with additions of H-X and  $\text{X}_2$  (X = F, Cl, Br, I) some of the first transformations of unsaturated molecules taught to students. Carbometallation is a widely used class of reaction that involves the addition of M-C (M = metal) across a double or triple C-C bond. One metal for which carbometallation has not been reported is beryllium. This is likely due to the highly toxic nature of most beryllium containing compounds, which has suppressed investigation of its fundamental chemistry in comparison to other elements.<sup>1</sup>

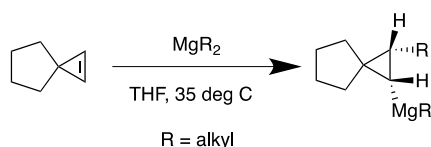
With beryllium compounds having the most covalent character out of any element in the s-block, the interaction of organoberyllium compounds with unsaturated organic species likely has a rich chemistry. Despite toxicity concerns, organoberyllium chemistry has been a topic of recent increasing attention.<sup>2-12</sup> It is therefore timely to investigate the potential for addition reactions of model diorganoberyllium species ( $\text{BeR}_2$ ) with model alkenes and alkynes (carboberyllation). Addition of diorganoberyllium to ene-ones is known, however organoberyllium species have not been isolated as the reactions are quenched as part of the workup.<sup>13, 14</sup>

It may be expected that carboberyllation with  $\text{BeR}_2$  has the most in common with the analogous and known carbometallation reactions with  $\text{BR}_3$  and  $\text{MgR}_2$ . The addition of an organoborane across double and triple bonds (carboboration) has been a reaction of increased interest in recent years.<sup>15, 16</sup> Typically, highly electrophilic boranes such as  $\text{B}(\text{C}_6\text{F}_5)_3$  have been employed and this reaction has been used to access a variety of otherwise difficult to synthesize boron-containing molecules, often in a single step.<sup>17</sup> For carboboration reactions, addition across the unsaturated CC bond generally occurs on the same side of the organic substrate (1,1-carboboration, Scheme 1), with 1,2-additions across the C-C multiple bond only rarely observed. In contrast, 1,2-addition is more typical with fundamental addition reactions (i.e. H-X, H-B).<sup>18-20</sup>



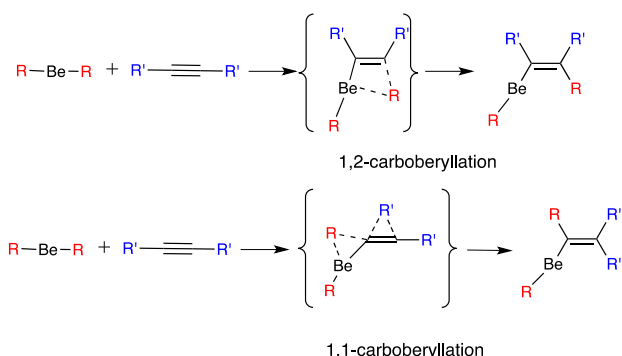
Scheme 1. Carboboration reaction between  $\text{B}(\text{C}_6\text{F}_5)_3$  and diphenyl acetylene.

For  $\text{MgR}_2$ , carbomagnesiation occurs via both 1,1 and 1,2 additions, but typically requires a metal catalyst to proceed (Scheme 2).<sup>21</sup> One uncatalyzed addition of  $\text{MgR}_2$  to a substituted cyclopropene has been reported.<sup>22</sup>



Scheme 2. Uncatalyzed carbomagnesiation of cyclopropenes.

Here we report the results of a computational investigation of the addition of  $\text{BeR}_2$  ( $\text{R} = -\text{Et}, -\text{Ph}, -\text{C}_6\text{F}_5$ ) to unsaturated C-C systems, with a comparison of 1,1 and 1,2 carbometallation on model internal alkenes, internal alkynes and phenylacetylene (Scheme 3). Thermodynamic and kinetic results and trends are compared to analogous transformations for  $\text{MgR}_2$  and  $\text{B}(\text{C}_6\text{F}_5)_3$ .



Scheme 3. Carboberyllation between dialkyl beryllium and alkynes.

## Computational Methods

Unless noted, all calculations were performed with Gaussian 09.<sup>23</sup> Geometry optimizations were carried out with the B3LYP density functional<sup>24, 25</sup> with the 6-311++G(d,p) basis set<sup>26, 27</sup> without any symmetry constraints. Stationary points were characterized as minima or transition states by calculating the Hessian matrix analytically. Frequency calculations indicate that all structures deemed minima had no imaginary frequencies and transition states exhibit one imaginary frequency. SCS-MP2<sup>28</sup> single-point energies were calculated with the same basis set at the gas-phase B3LYP geometries and modelled with solvent correction using the integral equation formulation of the polarizable continuum model (IEFPCM)<sup>29</sup> with Truhlar's SMD solvation model<sup>30</sup> and acetonitrile ( $\text{CH}_3\text{CN}$ ) solvent parameters. All SCS-MP2 reported  $\Delta G$  values are SCS-MP2 electronic energies with B3LYP/6-311++G(d,p) solvent correction and gas phase thermochemical corrections (standard conditions of  $T = 298.15$  K and  $p = 1$  atm). B3LYP/6-311++G(d,p) results for  $\Delta G$  are single point electronic energies (inclusive of solvent) with gas phase thermochemical corrections. Empirical dispersion was considered with B3LYP single-point energy calculations with D3 dispersion<sup>31</sup> and Becke-Johnson damping.<sup>32</sup> Transition state optimizations with B3LYP used the quadratic synchronous transit (QST) method.<sup>33</sup> Extensive analysis of intrinsic reaction coordinate (IRC) calculations ensured that the identified transition states correctly linked the associated minima.<sup>34</sup>

## Results and Discussion

We first investigated the energetics of addition of diorganoberyllium species to model alkenes and alkynes, with both 1,1 and 1,2 regioselectivity (Scheme 3). The diorganoberyllium species chosen were diethylberyllium and diphenylberyllium. Diethylberyllium is a model for dialkyl beryllium compounds, while diphenylberyllium is a species that is accessible for synthetic chemists.<sup>10</sup> The model alkenes considered were 2-butene and *E*-stilbene and the model alkynes were 2-butyne and diphenylacetylene. Results are presented in Table 1. For comparison, analogous reactions with organomagnesium compounds (carbomagnesiation) were considered, with results collated in Table 2.

There are significant differences in calculated reaction energies between the SCS-MP2 and B3LYP results. In general, the SCS-MP2 calculated free energy of reaction is more exergonic, favouring product formation. Importantly,  $\Delta G$  for all reactions is calculated to be exergonic with SCS-MP2, whereas B3LYP/6-311++G(d,p) predicts endergonic reactions for all reactions of  $\text{MEt}$  and  $\text{MPh}$  ( $\text{M} = \text{Be}, \text{Mg}$ ) with alkenes, and reactions with  $\text{Be}(\text{C}_6\text{F}_5)_2$ . Similarly, the SCS-MP2 calculated barrier heights are lower than those with B3LYP. Results with B3LYP-D3(BJ) are in much closer agreement with SCS-MP2 than B3LYP, which highlights the importance of van der Waals interactions in these system that are also present in part in MP2 calculations. It is expected that the SCS-MP2 and B3LYP-D3(BJ) results are more reliable than those with B3LYP, and will form the basis of subsequent discussion.

Table 1. Carboberyllation: B3LYP, B3LYP-D3(BJ), and SCS-MP2 calculated reaction free energies and barrier heights ( $\Delta G_{298\text{ K}}$ , kJ/mol), inclusive of acetonitrile solvent. 6-311++G(d,p) basis set results

Reactants	1,1-Carbometallation						1,2-Carbometallation					
	Reaction B3LY			Barrier B3LY			Reaction B3LY			Barrier B3LY		
	B3LY	P-	SCS-	B3LY	P-	SCS-	B3LY	P-	SCS-	B3LY	P-	SCS-
	P	D3(B J)	MP2	P	D3(B J)	MP2	P	D3(B J)	MP2	P	D3(B J)	MP2
BeEt <sub>2</sub> / <i>trans</i> -2-Butene	34	1	-11	244	216	232	33	0	-12	189	150	162
BeEt <sub>2</sub> / <i>E</i> -Stilbene	66	12	-22	278	239	243	48	2	-29	194	143	142
BeEt <sub>2</sub> /2-Butyne	-37	-69	-62	219	192	202	-37	-68	-64	154	117	146
BeEt <sub>2</sub> /Diphenylacetylene	-23	-76	-87	222	184	186	-32	-83	-95	163	113	133
BePh <sub>2</sub> / <i>trans</i> -2-Butene	41	2	-14	225	189	197	39	0	-19	179	132	134
BePh <sub>2</sub> / <i>E</i> -Stilbene	82	16	-21	268	216	206	56	0	-37	199	134	117
BePh <sub>2</sub> /2-Butyne	-44	-78	-77	211	178	181	-28	-69	-68	142	97	115
BePh <sub>2</sub> /Diphenylacetylene	-21	-85	-102	211	162	151	-21	-85	-102	161	97	102
BePh <sub>2</sub> /Phenylacetylene	-80	-100	-108	158	132	140	-65	-105	-105	134	83	100
Be(C <sub>6</sub> F <sub>5</sub> ) <sub>2</sub> /2-Butyne	-15	-52	-49	177	143	146	8	-32	-36	150	106	121
Be(C <sub>6</sub> F <sub>5</sub> ) <sub>2</sub> /Diphenylacetylene	13	-51	-71	173	127	114	17	-45	-67	161	100	100
B(C <sub>6</sub> F <sub>5</sub> ) <sub>3</sub> /Phenylacetylene	-55	-106	-117	129	93	73	-48	-106	-106	213	102	133
B(C <sub>6</sub> F <sub>5</sub> ) <sub>3</sub> /2-Butyne	-16	-73	-64	178	129	104	-23	-58	-83	196	137	129

Table 2. Carbomagnesiation: B3LYP, B3LYP-D3(BJ), and SCS-MP2 calculated reaction free energies and barrier heights ( $\Delta G_{298\text{ K}}$ , kJ/mol), inclusive of acetonitrile solvent. 6-311++G(d,p) basis set results.

Reactants	1,1-Carbometallation						1,2-Carbometallation					
	Reaction B3LY			Barrier B3LY			Reaction B3LY			Barrier B3LY		
	B3LY	P-	SCS-	B3LY	P-	SCS-	B3LY	P-	SCS_	B3LY	P-	SCS-
	P	D3(B J)	MP2	P	D3(B J)	MP2	P	D3(B J)	MP2	P	D3(B J)	MP2
MgEt <sub>2</sub> / <i>trans</i> -2-Butene	33	0	-10	272	250	260	36	3	-8	203	167	187
MgEt <sub>2</sub> / <i>E</i> -Stilbene	67	10	-15	303	272	275	34	-12	-41	198	148	145
MgEt <sub>2</sub> /2-Butyne	-36	-67	-61	249	226	232	-33	-64	-62	188	156	189
MgEt <sub>2</sub> /Diphenylacetylene	-17	-69	-82	241	207	206	-43	-94	-108	187	140	168
MgPh <sub>2</sub> / <i>trans</i> -2-Butene	37	-2	-12	258	230	240	47	3	-9	202	163	175
MgPh <sub>2</sub> / <i>E</i> -Stilbene	74	8	-19	296	255	247	52	-6	-36	205	144	129
MgPh <sub>2</sub> /2-Butyne	-46	-80	-77	235	209	212	-16	-56	-55	182	145	171
MgPh <sub>2</sub> /Diphenylacetylene	-23	-85	-99	232	192	187	-23	-85	-99	189	135	149

#### Additions of BeR<sub>2</sub> and MgR<sub>2</sub>

For 1,1-regioselective reactions the SCS-MP2 calculated  $\Delta G$  for Be and Mg reactions are nearly identical (maximum deviation of 7 kJ/mol), with a similar trend with B3LYP-D3(BJ) results (maximum deviation of 8 kJ/mol). Additions to C-C triple bonds are in general more favourable than addition to C-C double bonds, while addition of MPh is more favourable than MEt (M = Be, Mg). The transition state barriers with BeR<sub>2</sub> are in all cases very high, with the lowest being the addition of BePh<sub>2</sub> to alkynes, having barriers of 140-151 kJ/mol. The corresponding barriers for MgR<sub>2</sub> are generally 30-40 kJ/mol higher. Importantly, the results for these substrates indicate that 1,1-addition would not occur at experimentally reasonable temperatures for organometallic chemistry in any of the considered cases.

For 1,2-addition the calculated  $\Delta G$  of reaction is again similar between Be and Mg, with favourable thermodynamics in all cases. The barriers are significantly lower than for 1,1-addition. In general the barriers are higher for addition of Mg compared to Be, M-Et complexes give higher barriers than M-Ph, alkene barriers are higher than with alkynes, and alkyl substituents on the organic substrate give higher barriers than aryl substituents. Significantly, the calculated barrier for the 1,2-addition of BePh<sub>2</sub> to diphenylacetylene is the lowest of all reactions considered, being only 102 kJ/mol. The relatively low barrier is of a magnitude that could likely be overcome under typical reaction conditions, such as refluxing toluene, which is known to be compatible with organoberyllium species.<sup>5</sup> The addition of BePh<sub>2</sub> to the alkene *E*-stilbene with a barrier of 117 kJ/mol is also potentially feasible under reasonable experimental conditions.

### Comparison with Carboboration

To compare our results with the experimentally known 1,1-carboboration of alkynes with B(C<sub>6</sub>F<sub>5</sub>)<sub>3</sub> (as well as the experimentally rare 1,2-carboboration), we also calculated the thermodynamics and barrier heights for the 1,1- and 1,2- additions of B(C<sub>6</sub>F<sub>5</sub>)<sub>3</sub> with 2-butyne.<sup>35</sup> For this system, 1,2-addition is preferred thermodynamically with calculated  $\Delta G$  values of -64 and -83 kJ/mol for 1,1- and 1,2-addition, respectively. However, the calculated transition state barrier for 1,2-addition is substantially higher at 129 kJ/mol as compared to 104 kJ/mol for 1,1-addition, consistent with the experimental observation of 1,1-addition. The experimental conditions reported for the 1,1- reaction of Pr-CC-Pr and 4-octyne include refluxing in toluene for three days. The calculated thermodynamics for 1,1-addition are similar to that calculated for BePh<sub>2</sub> and diphenylacetylene with a 1,2-regioselectivity, which suggests that the proposed reaction with BePh<sub>2</sub> should be energetically feasible.

### Addition of BeR<sub>2</sub> to Terminal Alkyne

To evaluate the potential addition reaction of BeR<sub>2</sub> with a terminal alkyne, we opted to focus on the best scenario from the internal acetylene reactions, BePh<sub>2</sub>, with phenyl-substituted acetylene, Ph-CC-H (Scheme 3). The analogous reaction with B(C<sub>6</sub>F<sub>5</sub>)<sub>3</sub> proceeds with 1,1-regioselectivity, with migration of the H atom. The reaction is reported to proceed at room temperature over three hours.<sup>36, 37</sup> Consistent with experimental observations for B(C<sub>6</sub>F<sub>5</sub>)<sub>3</sub> we calculate a barrier of 73 kJ/mol for the 1,1-addition, with the unobserved 1,2-addition having a higher calculated barrier of 133 kJ/mol.

The 1,1- and 1,2-addition of BePh<sub>2</sub> to Ph-CC-H are both calculated to be thermodynamically favourable. The  $\Delta G$  is -108 kJ/mol for 1,1-addition and -104 kJ/mol for 1,2-addition. As in the addition to disubstituted acetylenes, the 1,2-addition is kinetically preferred for BePh<sub>2</sub> with the barrier for the 1,2-addition being 100 kJ/mol, compared with 140 kJ/mol for the 1,1-addition. A possible side reaction between Ph-CC-H and BePh<sub>2</sub> involves the deprotonation of the terminal acetylene with metallation giving an alkynylorganoberyllium,<sup>38, 39</sup> with formation of benzene. However, this reaction was found to be unfavourable with a calculated  $\Delta G$  of +18 kJ/mol.

### Addition of Be(C<sub>6</sub>F<sub>5</sub>)<sub>2</sub>

Ingleson and co-workers rationalize their observation of 1,2-addition for borenium cations vs the typical 1,1-addition for B(C<sub>6</sub>F<sub>5</sub>)<sub>3</sub> as being related to the migratory aptitude of the relative groups, with the C<sub>6</sub>F<sub>5</sub> group having a low migratory aptitude, thus favouring 1,1-regioselectivity.<sup>18</sup> To investigate whether the 1,2-reaction predicted for Be is related to the Be atom, we calculated the 1,1 and 1,2- additions of experimentally unknown Be(C<sub>6</sub>F<sub>5</sub>)<sub>2</sub> to diphenylacetylene. The calculated  $\Delta G$  is approximately 70 kJ/mol less favourable than the corresponding reaction with BePh<sub>2</sub>, but still exergonic by 71 and 67 kJ/mol for 1,1- and 1,2- reactions, respectively. The barrier to the 1,2-reaction is 14 kJ/mol lower than for the 1,1-reaction at

100 kJ/mol, consistent with the other cases for Be, indicating 1,2-regioselectively would be generally expected for carboberyllation reactions involving  $\text{BeR}_2$ .

### Comparison of Beryllium and Boron Metallation Pathways

As noted above, carboboration of alkynes with tris(pentafluorophenyl)borane typically affords a selective 1,1-addition reaction. Conversely, for organoberyllium our results indicate that 1,2-regioselectivity is expected for both terminal and internal acetylenes. Kehr and Erker<sup>15</sup> have reviewed 1,1-carboboration in great detail. In seeking to extend our understanding of the regioselective addition of carboboration and carboberyllation, we have probed the profile of the reaction energy pathway from IRC calculations in the neighbourhood of rate-determining steps of the overall reaction.

Results for the calculated pathways are presented in Table 1, with  $\Delta E$  relative energies plotted in Figures 1-3 (gas-phase B3LYP/6-311++G(d,p) calculated results, energies relative to separate reactants).

For carboberyllation the reaction of  $\text{BePh}_2$  with both phenylacetylene and diphenylacetylene was considered. The reaction between  $\text{BePh}_2$  and diphenylacetylene provides an excellent test case for examining the IRC energy profiles, as both 1,1 and 1,2 products exhibit the same atom-to-atom connectivity.

For the 1,1-addition mechanism of carboberyllation, the reaction profile highlights a two-step process, Figures 1 and 2. The first step occurs almost exclusively on the alkyne moiety, with a slow 1,2-R shift ( $\text{R}=\text{H}$ ,  $\text{Ph}$ ) across the C-C triple bond (a reorientation of the alkyne substituents). Moreover, the initial 1,2-shift across the alkyne is responsible for the reaction barrier height (maximum in energy profile). Upon completion of the first step, a secondary migration occurs with the Ph from diphenylberyllium migrating to the alkynyl carbon. This secondary rearrangement is characterised in Figures 1 and 2 by a point of inflexion, after which the energy profile rapidly goes downhill to the 1,1-substituted alkynylorganoberyllium products. From Figures 1-2, the  $\Delta E$  activation barriers for the 1,1-addition reaction of  $\text{Ph-CC-H}$  and  $\text{Ph-CC-Ph}$  with  $\text{BePh}_2$  are 116 and 152 kJ/mol, respectively (gas phase energies).

In the case of 1,2-addition (blue lines, Figures 1-2), the reaction energy profiles indicate a simple one-step process, with simultaneous coordination between the alkyne and organoberyllium and migration of Ph from the organoberyllium species to the alkyne. That is, simultaneous bond breaking between Be-Ph groups and bond reforming to the alkynyl carbon, leading to rapid formation of 1,2-substituted alkynylorganoberyllium products. Notably, at the transition state the interacting reactant complexes are favourably orientated for coordination. No secondary migration or substituent reorientation is noted in the energy profile. The predicted  $\Delta E$  barrier for the 1,2-reaction of  $\text{BePh}_2$  with phenylacetylene and diphenylacetylene is 42 kJ/mol and 68 kJ/mol, respectively.

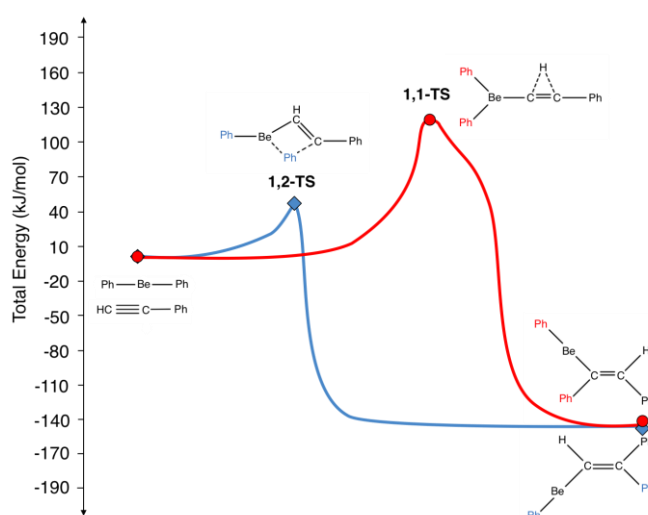


Figure 1. Carboberyllation: IRC energy profile for the reaction between  $\text{BePh}_2$  and phenylacetylene. B3LYP/6-311++G(d,p) calculated  $\Delta E$  relative energies (kJ/mol). 1,1-carboberyllation (red) and 1,2-carboberyllation (blue).

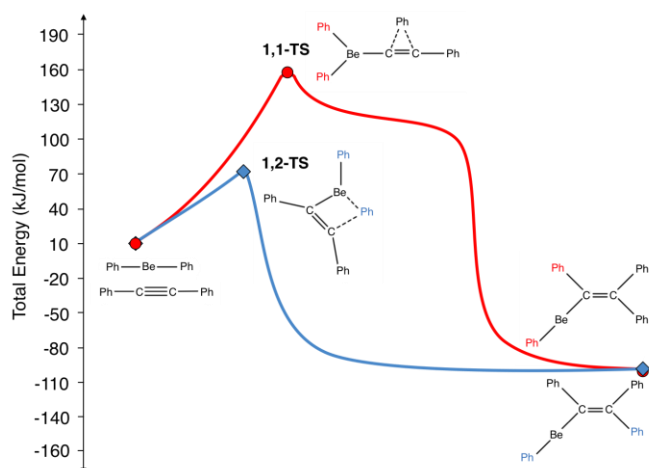


Figure 2. Carboberyllation: IRC energy profile for the reaction between  $\text{BePh}_2$  and diphenylacetylene. B3LYP/6-311++G(d,p) calculated  $\Delta E$  relative energies (kJ/mol). 1,1-carboberyllation (red) and 1,2-carboberyllation (blue).

For carboboration, the reaction energy profile of  $\text{B}(\text{C}_6\text{F}_5)_3$  with phenylacetylene was investigated, Figure 3. Our results indicate that the 1,1-addition mechanism of carboboration shares similar characteristics to that of carboberyllation. Again, the reaction profile indicates a two-step process. Analogous with 1,1-carboberyllation, the first step details a slow 1,2-R shift ( $\text{R}=\text{H}$ ) across the C-C triple bond. This initial 1,2-shift, exclusively occurring on

the alkyne moiety, again is responsible for the reaction barrier height, 92 kJ/mol. Secondary migration follows with the  $\text{C}_6\text{F}_5$  from tris(pentafluorophenyl) borane migrating to the alkynyl carbon. Distinctively, this secondary rearrangement is again characterised by a point of inflexion, after which the energy profile rapidly goes downhill to the 1,1-substituted alkenylborane product.

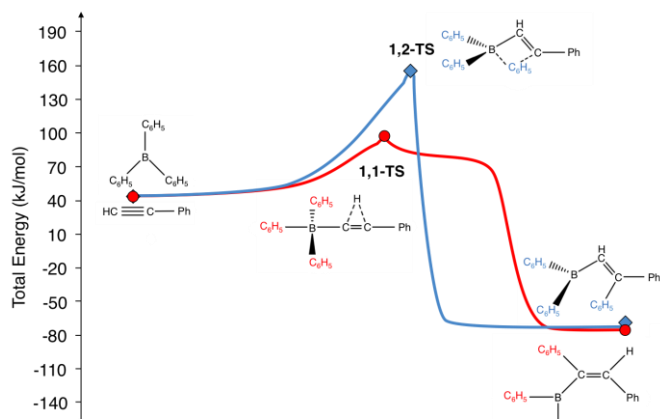


Figure 3. Carboboration: IRC energy profile for the reaction between  $\text{B}(\text{C}_6\text{F}_5)_3$  and phenylacetylene. B3LYP/6-311++G(d,p) calculated  $\Delta E$  relative energies (kJ/mol). 1,1-carboboration (red) and 1,2-carboboration (blue).

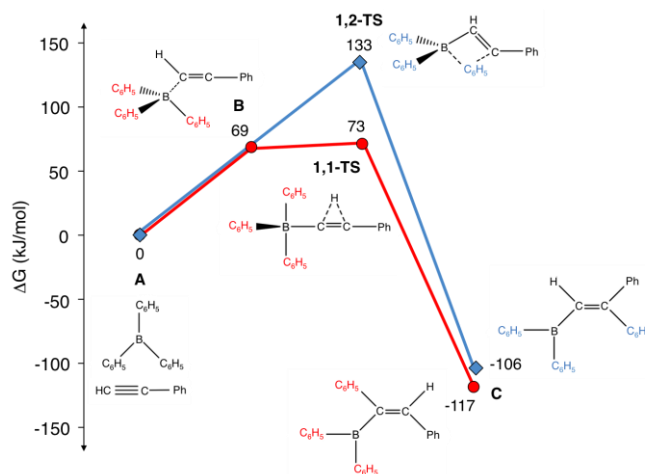
The reaction energy profile for 1,2-carboboration addition (blue line, Figure 3) is analogous to the 1,2-carboberyllation mechanism previously discussed. A one step process is evident, with simultaneous coordination between the alkyne and borane and migration of  $\text{C}_6\text{F}_5$  from the borane to the alkyne. No

secondary migration or substituent reorientation is noted in the energy profile. For carboboration, the  $\Delta E$  barrier for the 1,2-reaction with phenylacetylene is 152 kJ/mol, about 100 kJ/mol higher than the 1,2-carboberyllation barrier.

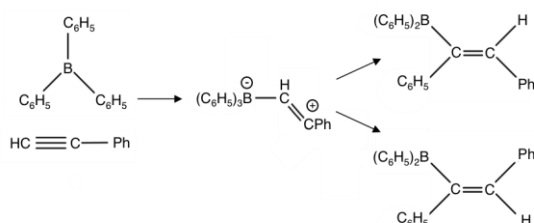
The DFT results for carboboration (Figure 3) are consistent with experimental observations of Kehr and Erker,<sup>15</sup> whereby the carboboration reaction of phenylacetylene with  $\text{B}(\text{C}_6\text{F}_5)_3$  occurred at room temperature and resulted in the selective formation of 1,1-carboboration products. The calculated  $\Delta E$  barrier of 92 kJ/mol for 1,1-carboboration addition is kinetically favourable compared to 1,2-addition (barrier of 152 kJ/mol).

From a previous theoretical investigation by Berke and co-workers<sup>37</sup> of 1,1-carboboration between  $\text{B}(\text{C}_6\text{F}_5)_3$  and phenylacetylene at the B3PW91/6-31+G(d) level of theory, it was suggested that 1,1-carboboration is facilitated by the means of a Wagner-Meerwein rearrangement and accelerated by respective local charges. The pathway proposed by Berke and co-workers for the formation of 1,1-carboboration is outlined in Scheme 4 and involves three key steps:

1. Formation of a  $\pi$ -adduct minimum between  $\text{B}(\text{C}_6\text{F}_5)_3$  and phenylacetylene



2. Migration of the hydrogen atom from the  $\eta$ -alkynic carbon to the  $\eta$ -alkynic carbon.
3. The highly electrophilic  $\eta$ -carbon of the intermediate becomes saturated by a boron to carbon  $\text{C}_6\text{F}_5$ -1,2-shift, completing the central  $\text{C}(\text{sp}_2)\text{--C}(\text{sp}_2)$  double bond.



Scheme 4. Proposed three-step mechanism for the reaction of  $\text{B}(\text{C}_6\text{F}_5)_3$  with phenylacetylene.<sup>37</sup>

Our current results for carboboration may be interpreted within this three-step reaction pathway, illustrated in Figure 4. At the B3PW91/6-31+G(d) level of theory, Berke located an intermediate  $\eta$ -type adduct complex between the reactants, with a bond distance between the boron atom and alkynic carbon of 1.749 Å. With B3LYP/6-

311++G(d,p) the interaction is slightly longer at 1.813 Å (**B**, Figure 5). The calculated B-C bond distances are larger than the sum of single-bond covalent radii (1.60 Å)<sup>40</sup> and the B3LYP calculated Wiberg bond index (WBI) value for the B-C bond in **B** is 0.600. The free energy of  $\eta$ -complex formation with B3PW91/6-31+G(d) and SCS-MP2/6-311++G(d,p) is 84 and 69 kJ/mol, respectively. The  $\eta$ -type adduct was characterised by Berke as a van de Waals interaction,<sup>37</sup> which is consistent with our present results.

Figure 4. SCS-MP2/6-311++G(d,p) calculated relative  $\Delta G$  (kJ/mol) for the 1,1-addition between  $\text{B}(\text{C}_6\text{F}_5)_3$  with phenylacetylene. 1,1-carboboration (red) and 1,2-carboboration (blue).

Adduct formation of  $\text{B}(\text{C}_6\text{F}_5)_3$ , as a strong electrophile (B charge in  $\text{B}(\text{C}_6\text{F}_5)_3$  is +0.86), at the  $\eta$ -C in  $\text{HCCPh}$  is consistent with the B3LYP calculated NPA charges, with -0.19 ( $\eta$ -C<sup>H</sup>) compared to -0.03 for the  $\eta$ -C<sup>Ph</sup>. No adduct was able to be located with the B bound to the  $\eta$ -C<sup>Ph</sup>.

From B3LYP/6-311++G(d,p) calculations, the **TS** associated with 1,1-carboboration involves hydrogen atom migration across the carbon-carbon triple bond. Subsequently, there is a minor energetic barrier of 4 kJ/mol from **B** to the **TS**, which initiates the reaction path to **C** (including rapid  $\text{C}_6\text{F}_5$  migration to the  $\eta$ -C). At the **TS**, the B-C bond contracts to 1.617 Å (WBI = 0.880) compared to **B**, consistent with a single-bond B-C description (sum of single-bond covalent radii is 1.6 Å).<sup>40</sup> At **C** the B-C bond is further shortened to 1.566 Å (WBI = 0.907), which is afforded stability with some B-C double bond character.

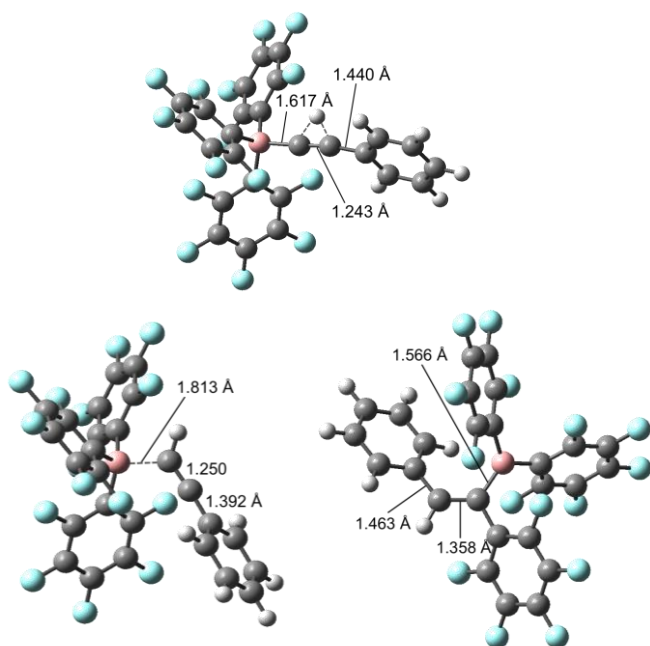




Figure 5. B3LYP/6-311++G(d,p) optimized geometries and selected calculated bond distances (Å) for the 1,1- addition between B(C<sub>6</sub>F<sub>5</sub>)<sub>3</sub> with phenylacetylene. Initial  $\pi$ -adduct **B** (bottom left), **TS** (top) and product **C** (bottom right).

Analysis of the reaction profile enabled identification of the rotation of the tris(pentafluorophenyl)borane moiety in the transition state pathway, in addition to tracking the stereochemical re-orientation about the boron to allow for secondary migration of the nucleophilic C<sub>6</sub>F<sub>5</sub> group. This step facilitates the energetic convergence to the 1,1-alkynylorganoboron product. Additionally, the nucleophilic migration of C<sub>6</sub>F<sub>5</sub> strongly depends on the electrophilic character of the B<sup>-</sup>C<sup>+</sup>=C(H)Ph intermediate complex. In accord with previous discussions, we agree the driving force for 1,1-carboboration relates to a Wagner-Meerwein shift where nucleophilic migration of the C<sub>6</sub>F<sub>5</sub> group affords the saturation of the electrophilic  $\alpha$ -alkynic carbon.

## Conclusions

Our results indicate that the addition of BePh<sub>2</sub> to alkenes may not occur under experimentally reasonable conditions for reactive organometallic species, with the lowest barrier being the 1,2-addition to E-stilbene at 117 kJ/mol. However the addition of BePh<sub>2</sub> to both terminal and internal acetylenes should be expected to occur with barriers of *ca.* 100 kJ/mol. Reactions with organoberyllium species having similar calculated barriers have been observed to occur under typical conditions such as a few hours in refluxing toluene.<sup>5, 41</sup> It is predicted that for both terminal and internal acetylenes a 1,2-regioselectivity of the addition is expected, in contrast to the carboboration reactions. We hope that chemists competent in safely handling organometallic Be complexes will be able to validate our predictions, as well as find use for this class of reaction in generating new organometallic Be molecules.

## Acknowledgements

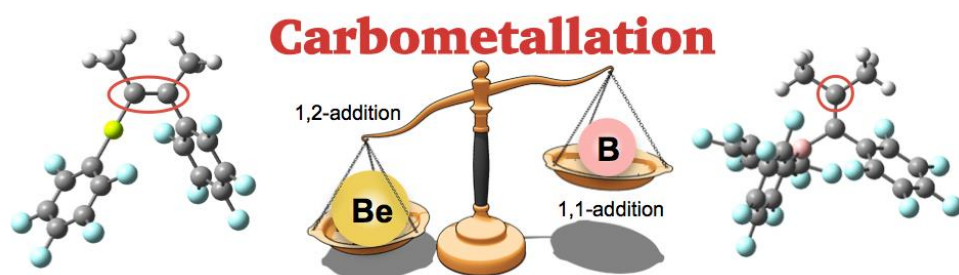
This work was generously supported by The Australian Research Council (JLD; FT160100007, DW; DP160103046) and La Trobe University. We thank La Trobe University, NCI and Intersect for computing resources.

## References

1. B. L. Scott, T. M. McCleskey, A. Chaudhary, E. Hong-Geller and S. Gnanakaran, *Chem. Commun.*, 2008, 2837-2847.
2. D. Naglav, M. R. Buchner, G. Bendt, F. Kraus, S. Schulz, *Angew. Chem. Int. Ed.* 2016, **55**, 10562-10576.
3. K. J. Iversen, S. A. Couchman, D. J. D. Wilson and J. L. Dutton, *Coord. Chem. Rev.*, 2015, **297-298**, 40-48.
4. M. Arrowsmith, H. Braunschweig, M. A. Celik, T. Dellermann, R. D. Dewhurst, W. C. Ewing, K. Hammond, T. Kramer, I. Krummenacher, J. Mies, K. Radacki, J. K. Schuster, *Nat. Chem.* 2016, **8**, 890-894.
5. M. Arrowsmith, M. S. Hill, G. Kociok-Köhn, D. J. MacDougall and M. F. Mahon, *Angew. Chem. Int. Ed.*, 2012, **51**, 2098-2100.
6. M. Arrowsmith, M. S. Hill and G. Kociok-Köhn, *Organometallics*, 2015, **34**, 653-662.
7. S. C. Chmely, T. P. Hanusa and W. W. Brennessel, *Angew. Chem. Int. Ed.*, 2010, **49**, 5870-5874.
8. S. A. Couchman, N. Holzmann, G. Frenking, D. J. D. Wilson and J. L. Dutton, *Dalton Trans.*, 2013, **42**, 11375-11384.
9. R. J. Gilliard, M. Y. Abraham, Y. Wang, P. Wei, Y. Xie, B. Quillian, H. F. Schaefer, P. v. R. Schleyer and G. H. Robinson, *J. Am. Chem. Soc.*, 2012, **134**, 9953-9955.
10. J. Gottfriedsen and S. Blaurock, *Organometallics*, 2006, **25**, 3784-3786.
11. W. Petz, K. Dehnicke, N. Holzmann, G. Frenking and B. Neumüller, *Z. Anorg. Allge. Chem.*, 2011, **637**, 1702-1710.
12. P. Parameswaran and S. De, *Dalton Trans.*, 2013, **42**, 4650-4656.
13. H. Gilman and R. H. Kirby, *J. Am. Chem. Soc.*, 1941, **63**, 2046-2048.



14. A. Krief, M. J. de Vos, S. De Lombart, J. Bosret and F. Couty, *Tet. Lett.*, 1997, **38**, 6295-6298.
15. G. Kehr and G. Erker, *Chem. Commun.*, 2012, **48**, 1839-1850.
16. R. L. Melen, *Chem. Commun.*, 2014, **50**, 1161-1174.
17. G. Kehr and G. Erker, *Chem. Sci.*, 2016, **7**, 56-65.
18. I. A. Cade and M. J. Ingleson, *Chem. Eur. J.*, 2014, **20**, 12874-12880.
19. R. L. Melen, L. C. Wilkins, B. M. Kariuki, H. Wadepohl, L. H. Gade, A. S. K. Hashmi, D. W. Stephan and M. M. Hansmann, *Organometallics*, 2015, **34**, 4127-4137.
20. M. Devillard, R. Brousses, K. Miqueu, G. Bouhadir and D. Bourissou, *Angew. Chem. Int. Ed.*, 2015, **54**, 5722-5726.
21. K. Murakami and H. Yorimitsu, *Beil. J. Org. Chem.*, 2013, **9**, 278-302.
22. E. K. Watkins and H. G. Richey Jr, *Organometallics*, 1992, **11**, 3785-3794.
23. M. J. Frisch, G. W. Trucks, H. B. Schlegel, G. E. Scuseria, M. A. Robb, J. R. Cheeseman, G. Scalmani, V. Barone, B. Mennucci, G. A. Petersson, H. Nakatsuji, M. Caricato, X. Li, H. P. Hratchian, A. F. Izmaylov, J. Bloino, G. Zheng, J. L. Sonnenberg, M. Hada, M. Ehara, K. Toyota, R. Fukuda, J. Hasegawa, M. Ishida, T. Nakajima, Y. Honda, O. Kitao, H. Nakai, T. Vreven, J. A. M. Jr., J. E. Peralta, F. Ogliaro, M. Bearpark, J. J. Heyd, E. Brothers, K. N. Kudin, V. N. Staroverov, T. Keith, R. Kobayashi, J. Normand, K. Raghavachari, A. Rendell, J. C. Burant, S. S. Iyengar, J. Tomasi, M. Cossi, N. Rega, J. M. Millam, M. Klene, J. E. Knox, J. B. Cross, V. Bakken, C. Adamo, J. Jaramillo, R. Gomperts, R. E. Stratmann, O. Yazyev, A. J. Austin, R. Cammi, C. Pomelli, J. W. Ochterski, R. L. Martin, K. Morokuma, V. G. Zakrzewski, G. A. Voth, P. Salvador, J. J. Dannenberg, S. Dapprich, A. D. Daniels, Ö. Farkas, J. B. Foresman, J. V. Ortiz, J. Cioslowski and D. J. Fox, *Gaussian 09*, (2009) Gaussian, Inc., Wallingford CT.
24. A. D. Becke, *Phys. Rev. A*, 1988, **38**, 3098.
25. C. Lee, W. Yang and R. G. Parr, *Phys. Rev. B*, 1988, **37**, 785.
26. A. D. McLean and G. S. Chandler, *J. Chem. Phys.*, 1980, **72**, 5639.
27. K. Raghavachari, J. S. Binkley, R. Seeger and J. A. Pople, *J. Chem. Phys.*, 1980, **72**, 650.
28. S. Grimme, *J. Chem. Phys.*, 2003, **118**, 9095.
29. J. Tomasi, B. Mennucci and E. Cancès, *J. Mol. Struct. (Theochem.)*, **1999**, 464.
30. A. V. Marenich, C. J. Cramer and D. G. Truhlar, *J. Phys. Chem. B*, 2009, **113**, 6378-6396.
31. S. Grimme, J. Antony, S. Ehrlich and H. Krieg, *J. Chem. Phys.*, 2010, **132**, 154104.
32. S. Grimme, S. Ehrlich and L. Goerigk, *J. Comp. Chem.*, 2011, **32**, 1456-1465.
33. C. Peng and H. B. Schlegel, *Israel J. Chem.*, 1993, **33**, 449-454.
34. K. Fukui, *Acc. Chem. Res.*, 1981, **14**, 363.
35. C. Chen, G. Kehr, R. Fröhlich and G. Erker, *J. Am. Chem. Soc.*, 2011, **132**, 13594-13595.
36. C. Chen, T. Voss, R. Fröhlich, G. Kehr and G. Erker, *Org. Lett.*, 2011, **13**, 62-65.
37. C. Jiang, O. Blacque and H. Berke, *Organometallics*, 2010, **29**, 125-133.
38. N. A. Bell, I. W. Nowell, G. E. Coates and H. M. M. Shearer, *J. Organomet. Chem.*, 1984, **273**, 179-185.
39. B. Morosin and J. Howatson, *J. Organomet. Chem.*, 1971, **29**, 7-14.
40. P. Pyykkö and M. Atsumi, *Chem. Eur. J.*, 2009, **15**, 186-197.
41. K. J. Iversen, D. J. D. Wilson and J. L. Dutton, *Organometallics*, 2013, **32**, 6209-6217.



TOC Synopsis: A theoretical evaluation of the unknown addition of diorganoberyllium to model alkenes and alkynes (carboberyllation) shows the reaction with alkynes should be feasible. In contrast with carboboration a 1,2- regioselectivity is predicted.